JPET Fast Forward. Published on October 8, 2024 as DOI: 10.1124/jpet.124.002238
This article has not been copyedited and formatted. The final version may differ from this version.

The protective effect of irisin against hemorrhagic injury is mediated by PI3K and p38 pathways in hemorrhage/resuscitation.

Huai Wen[1], Naohiro Yano[1], Thomas Zhao[3], Lei Wei[4], Ting C Zhao[1,2]

[1]Department of Surgery and [2]Department of Plastic Surgery, Rhode Island Hospital, Warren Alpert Medical School of Brown University, Providence, RI. [3] Department of Biology, Boston University, Boston, MA. [4]Department of Orthopedics, Rhode Island Hospital, Brown University, Providence, RI.

Runing title: PI3K, p38 and irisin in hemorrhage/resuscitation

Corresponding Author:
Ting C Zhao, MD, Professor, Department of Surgery, Rohde Island Hospital, Warren Alpert Medical School of Brown University, Providence, RI 02903. Email: Ting_Zhao@Brown.Edu; Tel: 401-4447237; Fax:401-4445716

Total Pages: 31
Tables:1
Figures: 8
References: 82
Words: 9127
Abstract: 220
Introduction words:750
Discussion words:1294

Abbreviations

DMSO, dimethyl sulfoxide**; EDV,** end-diastolic volume**; EF**, Ejection Fraction; **ELISA,** enzyme linked immunosorbent assay**; FNDC5,** fibronectin type III domain-containing protein 5**; FS**, Fraction Shortening; **H&E,** hematoxylin and eosin**; H/R,** hemorrhage and resuscitation**; HR**, Heart Rate; **IL6,** interleukin-6**; IVSd**, LV Interventricular Septal thickness in diastole; **IVSs**, LV Interventricular Septal thickness in systole; **LVIDd**, LV Internal Dimension in diastole; **LVIDs**, LV Internal Dimension in systole; **LVPWd**, LV Posterior Wall thickness in diastole; **LVPWs**, LV Posterior Wall thickness in systole; **LVvold/EDV**, Left ventricular volume in diastole; **LVvols/ESV**, Left ventricular volume in systole; **MAPK,** mitogen-activated protein kinase**; MODS,** multiple organ dysfunction syndrome**; PI3K,** phosphoinositide 3-kinase**; PBS,** phosphate-buffered saline**;**

JPET Fast Forward. Published on October 8, 2024 as DOI: 10.1124/jpet.124.002238
This article has not been copyedited and formatted. The final version may differ from this version.

SIRS, systemic inflammatory response syndrome**; TNF-*α*,** tumor necrosis factor alpha**; TUNEL,** Terminal Deoxynucleotidyl Transferase dUTP Nick End Labeling

Section: Cardiovascular

ABSTRACT

The objective of this study is to investigate whether PI3kinase (PI3K) and p38 mitogen-activated kinase contributes to the protection of irisin during hemorrhage/resuscitation. Experimental groups were divided by receiving the different treatments during resuscitation: **I**) Hemorrhage: Adult male CD-1 mice were subjected to hemorrhage at a mean arterial blood pressure of 35~45 mmHg for 60 min followed by 120 min of resuscitation (n=13); **II**) Hemorrhage + Irisin: receiving irisin (5μg/kg) (n=13); **III**) Hemorrhage + Irisin + PI3K inhibitor: receiving both Ly294002 (1mg/kg, i.v.) and irisin (n=6); **IV**) Hemorrhage + Irisin + p38 inhibitor: receiving SB202190 (1mg/kg, i.v.) and irisin (n=6). Compared to hemorrhage/resuscitation control, irisin improved cardiac function and the recovery of hemodynamics in association with the decreased systemic IL-1, IL-6, and TNF-α, which was completely abrogated by PI3K or p38 inhibitions. Furthermore, the inhibition of PI3K or p38 abolished irisin-induced the reduction of the inflammatory cell infiltration and TUNEL-positive apoptosis in the cardiac and skeletal muscles. Irisin reduced TNF-α and IL6 expression in cardiac and skeletal muscles, which was abrogated by the inhibition of PI3K or p38. Irisin-treated hemorrhage increases the phosphorylation of PI3K and p38 in both cardiac and skeletal muscles, which was mitigated by the inhibition of PI3K or p38**. Conclusion:** PI3K and p38 play an important role in modulating the protective effect of irisin during the hemorrhage/resuscitation.

Key Words: Hemorrhage/resuscitation; Tissue injury; Irisin; PI3K; p38 MAPK; Cardiac function; Hemodynamics.

JPET Fast Forward. Published on October 8, 2024 as DOI: 10.1124/jpet.124.002238
This article has not been copyedited and formatted. The final version may differ from this version.

SIGNIFICANCE STATEMENT

This study has identified a critical pathway in the regulation of trauma/hemorrhage by using a preclinical trauma model, in which Irisin, as a hormone factor, stimulates PI3 Kinase and p38 pathways to induce protection against traumatic conditions.

The study holds promise for developing a new therapeutic strategy to target irisin and its pathways related to PI3K and p38 to treat trauma and its comorbidities to reduce mortality for clinical implications.

INTRODUCTION

Hemorrhagic shock, a life-threatening condition characterized by rapid and substantial blood loss leading to organ hypoperfusion, is a frequent medical emergency (Gruen et al., 2012). Despite hemodynamic stabilization being achieved through fluid resuscitation, survivors of hemorrhage and resuscitation (H/R) have a tendency to develop systemic inflammatory response syndrome (SIRS), which can lead to multiple organ dysfunction syndrome (MODS) and even death (Jarrar et al., 1999; Gruen et al., 2012). While managing hemorrhage has dramatically improved, it remains a significant global health challenge (Cannon, 2018). Medical comorbidities are prevalent in patients with hemorrhage/trauma (Andaluz and Zuccarello, 2009). The previous studies revealed a close correlation between hemorrhage and the development of post-traumatic stress disorder (Tang et al., 2023; Deniau B et al., 2024). There is a close connection between additional comorbidities and hemorrhage/traumatic injury with an increased mortality (Shoko et al., 2010; El Ayadi et al., 2013). Thus, the identification of new mechanisms in trauma will provide important information for developing therapeutic strategies for treatment of trauma and comorbid conditions.

JPET Fast Forward. Published on October 8, 2024 as DOI: 10.1124/jpet.124.002238
This article has not been copyedited and formatted. The final version may differ from this version.

Cardiac dysfunction contributes critically to the development of multiorgan failures and the mortality of patients, who initially survived hemorrhagic shock (Simpson et al., 2023). A normal myocardial response could manifest an elevated cardiac output at early phases of hemorrhage, but can lead to a dramatic decrease over a short period (Wall et al., 2019; Gutierrez et al., 2004). The existence of trauma-elicited cardiovascular damage is related to poor patient outcomes (Wilson et al., 2017). Thus, the study of pathways for modulating hemorrhage-induced cardiac dysfunction will provide an important clue for understanding and developing therapeutic strategies. Amidst the search for ideal treatments for H/R injury, irisin, as a myokine, emerges as a particularly intriguing candidate (Wang et al., 2020b; Wang et al., 2023b). Irisin is produced through the proteolytic cleavage of the N-terminal fragment of fibronectin type III domain-containing protein 5 (FNDC5), which plays an important role in the regulation of physiological function (Bostrom et al., 2012; Jedrychowski et al., 2015; Liu et al., 2022;) and contributes to mitigating inflammation, combating insulin signaling, and tissue injury (Mazur-Bialy et al., 2017; Wang et al., 2020a; Wang et al., 2020b; Wang et al., 2017). Lack of irisin manifests metabolic derangement (Luo et al., 2020) whereas increased plasma irisin is linked to adiposity in type II diabetes mellitus (Rana et al., 2017*)*. Irisin serves as a biomarker for cardiovascular disease in association with cardiometabolic health (Liu et al., 2022; Almeida et al., *2023)* and the suppression of osteoblastic transformation of vascular smooth muscle cells (Wang et al., 2020*)*. Lower concentrations of irisin were correlated with longer rehabilitation time in COVID infected patients (Mińko et al., 2024; Alves et al., 2024). Our recent studies indicate that irisin improves cardiac function in H/R (Kulthinee et al., 2022; Wang et al., 2023b). However, the precise mechanisms by which irisin functions in hemorrhage/resuscitation scenarios remain to be fully elucidated.

JPET Fast Forward. Published on October 8, 2024 as DOI: 10.1124/jpet.124.002238
This article has not been copyedited and formatted. The final version may differ from this version.

The phosphoinositide 3-kinases (PI3Ks) are essential in the regulation of survival and inflammatory responses (Cantley, 2002), manifesting critical functionality in trauma (Cai and Semenza, 2004; Tsai et al., 2012; Durrant and Hers, 2020). Activation of PI3K was linked to survival in lethal hemorrhagic shocks (Hwabejire et al., 2014). Pharmacological inhibition of PI3K attenuated the protection against cardiac damage and proinflammation in trauma-hemorrhage (Liu et al., 2012). Notably, the PI3K pathway co-ordinates with FNDC5 to regulate ischemia-reperfusion injury (Zhou et al., 2024). Nevertheless, it remains unknown whether PI3K contributes critically to the regulation of irisin's protection during hemorrhage-resuscitation.

p38 mitogen-activated protein kinase (MAPK) is a critical contributor to the regulation of tissue injury (Roux and Blenis, 2004). Pharmacologic activation of p38 triggers delayed cardioprotection (Zhao et al., 2001a; Zhao et al., 2001b; Zhao et al., 2013). Irisin inhibited neutrophil extracellular trap formation in acute pancreatitis via P38 pathway (Han et al., 2023). Irisin combats hypertension and vascular damage in angiotensin II challenged mice through the suppression of p38 (Huang et al., 2022). Inhibition of p38 activity prevented the attenuated proinflammatory responses and hepatic injury in hemorrhagic shock (Liu et al., 2011). However, whether p38 plays a critical role into irisin-induced protection against hemorrhagic injury during hemorrhage/resuscitation remains to be determined.

In this study, we assess whether PI3K and p38 in association with irisin can contribute to the development of protection in hemorrhage/resuscitation. Our findings reveal that recombinant irisin-elicited profound protective effects against hemorrhagic injury and were abrogated by the inhibition of PI3K and p38 pathways. This indicated that irisin mediated PI3K and P38 pathways are

JPET Fast Forward. Published on October 8, 2024 as DOI: 10.1124/jpet.124.002238
This article has not been copyedited and formatted. The final version may differ from this version.

critical to achieving protective effects in H/R.

MATERIALS AND METHODS

1. Animals: Male CD-1 mice, 8 weeks (25 ~ 30 g), were purchased from Charles River Laboratories (Wilmington, MA, USA). Mice were housed in a 12:12 hour light-dark cycle at a constant temperature and humidity-controlled room with free access to food and water for a minimum of three days before experiments. Experimental procedures were carried out under a protocol approved by the Institutional Animal Care and Use Committee of the Institute, which complies with National Institutes of Health "the Guide for the Care and Use of Laboratory Animals (NIH Publication No. 85-23, revised 1996)".

2. Reagents and antibodies: Recombinant human irisin was obtained from Cayman Chemical (Michigan, USA). Other chemicals were purchased from Sigma-Aldrich (St. Louis, MO). The assay kits for Terminal deoxynucleotidyl transferase nick-end labeling (TUNEL) were purchased from Millipore-Sigma (Burlington, MA, USA). PI3 kinase inhibitor Ly294002 was obtained from Sellechechem and P38 MAPK inhibitors SB202190 was obtained from Sigma-Aldrich (St. Louis, MO). Poly-clonal rabbit antibodies against phosphorylated p38 (Catalog: 9211), non-phosphorylated p38 (Catalog: 9212), phosphorylated PI3 submit p85 (Catalog: 4228), non-phosphorylated subunit 85 (Catalog: 4292) were obtained from Cell Signaling Technology (Boston, MA, USA). Goat anti-rabbit IgG (H+L) secondary antibody, HRP (Catalog: 31460) was obtained from ThermoFisher Scientific (Waltham, MA).

3. Hemorrhagic shock/resuscitation protocol: The Hemorrhagic Shock/Resuscitation injury model utilized in this study is based on our established protocols as previously described (Kulthinee et al.,

JPET Fast Forward. Published on October 8, 2024 as DOI: 10.1124/jpet.124.002238
This article has not been copyedited and formatted. The final version may differ from this version.

2022). Anesthesia was induced by administering 4% and maintaining with 1-2% isoflurane in oxygen to the animals. Mice were then carefully placed in a supine position on a temperature-controlled surgical pad, maintained at a precise 37~38°C, and transferred to a nose cone setup. The surgical procedure entailed the meticulous isolation of femoral arteries, followed by the insertion of PE-10 tubing that was connected to PE-50 tubes filled with heparinized saline. Hemorrhagic shock was induced through a controlled withdrawal of blood from the right femoral artery catheter to reduce the mean arterial pressure (MAP) to maintain 35~45 mmHg. Simultaneously, the left femoral artery catheter was connected to a physiological pressure transducer MLT844 (ADInstruments, INC, Colorado Springs, CO), enabling MAP recording. These measurements were continuously monitored using the Power Lab Data Acquisition system (Adinstruments, Colorado Spring, CO). Throughout the shock phase, meticulous adjustments involving additional blood withdrawal or reinfusion were made to maintain the MAP within the desired range (35~45 mmHg). After enduring 60 minutes of shock, the mice underwent a carefully timed resuscitation process. This entailed administering a volume triple that of the extracted blood, which included both the withdrawn blood and lactated Ringer's solution (LRS). The resuscitation was performed via a catheter of the right femoral artery over 15 minutes, using a sterilized syringe to ensure a controlled and gradual recovery.

4. **Experimental treatment protocol:** The hemorrhage/resuscitation on mice protocol was conducted as outlined above and shown in **Figure 1** and below, in which each group consisted of pharmacologic treatment and assay of post-resuscitation. Drug treatments were administered at the early phase of resuscitation via intravenous injection, which included recombinant Irisin (5 μg/kg body weight, i.v.), Ly294002, a PI3 Kinase inhibitor (1mg/kg body weight, i.v.), and SB202190, and a P38 MAPK inhibitor SB202190 (1mg/kg body weight, i.v.). Irisin was dissolved in phosphate-buffered saline

JPET Fast Forward. Published on October 8, 2024 as DOI: 10.1124/jpet.124.002238
This article has not been copyedited and formatted. The final version may differ from this version.

(PBS), Ly294002 and SB202190 were prepared in dimethyl sulfoxide (DMSO). The experimental groups were divided as follows: Group I) **Hemorrhage**: mice were subjected to hemorrhage for 60 minutes followed by resuscitation; Group II) **Hemorrhage + Irisin**: mice were subjected to an identical surgical protocol as Group I except the recombinant irisin (5μg/kg) was intravenously infused at the onset of resuscitation; Group III) **Hemorrhage + Irisin + Ly294002**: the same as Group II except that Ly294002 (1mg/kg, i.v.) and irisin were simultaneously infused during resuscitation; Group IV) **Hemorrhage + Irisin + SB202190**: the same as the Group II except that SB202190 (1mg/kg, i.v.) and irisin were simultaneously infused during resuscitation. After the end of hemorrhage/resuscitation and completion of the echocardiographic analysis, the mice were humanely euthanized, following which blood samples, as well as skeletal muscle and cardiac tissues, were meticulously collected for further analysis.

5. **Hemodynamics measurement and echocardiography:** As previously detailed in the section describing the H/R model, the mean arterial pressure was continuously captured using the Power Lab Data Acquisition system. Following a 5-minute stabilization period after successful intubation, the baseline of MAP values was recorded to establish a reference point for subsequent analyses.

Echocardiographic assessments were performed on the mice at 2 hours post-surgery, utilizing the advanced Philips CX50 ultrasound system connected with an L15-7io linear array transducer (Philips, Cambridge, MA, USA) to evaluate left ventricular (LV) function. The procedure was conducted under anesthesia through the continuous inhalation of 1~4% isoflurane mixed with oxygen. Subsequently, the mice were positioned in a supine posture on a warm pad to maintain body temperature. The precordial region was delicately prepared by removing any hair, followed by the application of ultrasound transmission gel that was pre-warmed (Aquasonic, Parker Laboratory,

JPET Fast Forward. Published on October 8, 2024 as DOI: 10.1124/jpet.124.002238
This article has not been copyedited and formatted. The final version may differ from this version.

Fairfield, NJ, USA) to ensure optimal image quality. The focus was then set on the LV's short axis to obtain detailed two-dimensional B-mode images and M-mode tracings at a position of the papillary muscles. For a comprehensive assessment, three to six consecutive cardiac cycles were recorded and analyzed using CX50 system equipped cardiac calculation software. Measurements were performed by an experienced operator, adhering to a double-blinded protocol to ensure unbiased and accurate results.

6. Enzyme-linked immunosorbent assay (ELISA) for measurement of systemic cytokines: Serum concentrations of IL-1, IL-6 (R&D Systems, Minneapolis, MN), and TNF-α Biolegend (San Diego, CA) were measured by using an ELISA kit. Following the manufacturer's protocol, 96-well microplates were coated with the diluted capture antibody (100 µL per well). Coated plates were sealed and incubated overnight at 4^0C. After washing, plates were blocked by adding 200-300 µL of blocking buffer and incubated for a minimum of one hour at room temperature. After washing 4 times, standards or samples (100 µL per well) were added to the appropriate wells, and incubated at room temperature for 2 hours with shaking. Detection antibody solution was then added to each well and further incubated at RT for 1-2 hours with shaking. Following streptavidin-HRP was added to each well for 30 minutes, and then the plates were washed. TMB substrate solution was added to each reaction, and the reaction was stopped by adding stop solution to each well, cytokine levels were determined from 450 nm absorbance readings with a SpectraMax M2e Microplate Reader (Molecular Device, San Jose, CA,).

7. Histological analysis and Immunohistochemistry: Skeletal muscles (gastrocnemius muscles, GAS) and heart tissues were harvested at the end of experiments and fixed in 10% formalin for 24 to 48 hours. They were processed, embedded, and then sectioned into 5 µm slices. Following

JPET Fast Forward. Published on October 8, 2024 as DOI: 10.1124/jpet.124.002238
This article has not been copyedited and formatted. The final version may differ from this version.

deparaffinization with xylene, the sections underwent a serial gradient alcohol rehydration process. The tissue sections were stained with hematoxylin and eosin, followed by dehydration with alcohol and xylene and coverslip slides using Permount. Also, the tissue sections were then counterstained with 5% methyl green solution for immunohistochemistry. Slides were visualized using a NikonEclipse Model Ni-E microscope, and images were captured with a Nikon Camera DS-RI color camera under 20x high power with a plan apo (20x/0.75) using NIS-element digital imaging software. Photomicrographs of 6 random fields per section for three sections were taken to obtain 18 fields from individual heart and/or muscle tissue and analyzed with NIH Image J software.

The scoring of muscle damage and infiltration of inflammatory cells was done in a double-blind manner for unbiased results, which is based on the grade 1-4 of inflammation in tissues: 1: No significant changes; 2: Scattered, random inflammatory cells; 3: Moderately mixed inflammatory cells; 4: Clusters of mixed inflammatory cells.

8.Terminal deoxynucleotidyl transferase dUTP nick end labeling (TUNEL): Millipore's ApopTag® Detection Kit (S7100, Millipore, USA) was used to perform the TUNEL assay. Slides were deparaffinized, dehydrated, and treated with proteinase K, followed by hydrogen peroxide to Quench Endogenous Peroxidase. After washing and equilibration, sections were incubated with TdT enzyme and anti-digoxigenin conjugate, each for 1 hour. Post-staining with peroxidase substrate and counterstaining with methyl green, slides were rehydrated and mounted, and viewed under microscope at high power 20X. Apoptotic cells were quantified by counting TUNEL-positive nuclei, which was done by a blinded investigator. Likewise, six random fields per section for three sections were taken to obtain 18 fields from individual heart and/or muscle tissue using a light microscope and analyzed with NIH ImageJ.

JPET Fast Forward. Published on October 8, 2024 as DOI: 10.1124/jpet.124.002238
This article has not been copyedited and formatted. The final version may differ from this version.

9. Quantitative real-time polymerase chain reaction (q-PCR): Total RNA was extracted and purified from skeletal muscle and heart by using a RNeasy mini kit (QIAGEN, GmbH, D-40724 Hilden, Germany). cDNA was synthesized from the amount of 2µg of total tissue RNA. Experiments for real-time PCR were conducted on a CFX connect real time PCR detection system (Bio-Rad) using qPCR kit kapa SYBR fast master mix (Kapabiosystems, Boston, USA). Primers used in the studies are as follows: IL1 β forward: 5- AAATGCCACCTTTTGACAGTGA -3; Reverse: 5- CATCTCGGAGCCTGTAGTGC -3. TNFα forward:5- AGGCACTCCCCCAAAAGATG-3; Reverse: 5- CCACTTGGTGGTTTGTGAGTG-3. GAPDH was included as the internal control: Forward: 5- GGAGAGTGTTTCCTCGTCCC -3; Reverse: 5- ACTGTGCCGTTGAATTTGCC -3. The reaction volume was 20 µl per sample. The expression of transcriptions was normalized to GAPDH levels. Results are reported using the $2^{-\Delta\Delta CT}$ method.

10. Western blot analysis: The extraction of protein and western blot for assessment of protein expression were performed as described previously (Zhao et al., 2007). Briefly, myocardial tissues and gastrocnemius muscles (GAS) were isolated and then homogenized in cold lysis buffer containing protease inhibitor cocktails (Sigma-Aldrich, St. Louis, MO). The Protein lysates were incubated at 4℃ for 30min under shaking. The supernatants of these samples were obtained via centrifugation at 12,000 g at 4℃ for 20 minutes. The protein content was measured with a Micro BCA Assay Kit (Thermo Scientific, Rockford, IL). 25µg protein was loaded into wells of Bis-Tris gel. After running and transferring, the membranes were blocked for 1 h at room temperature with 5% milk in PBST. The membranes were incubated with each primary polyclonal antibody, which includes phosphorylated PI3K, and phosphorylated p38 MAPK, PI3K, p38 MAPK (Cell Signaling Technology, Danvers, MA) at a concentration of 1:1000 dilution at 4℃ overnight with shaking. The

JPET Fast Forward. Published on October 8, 2024 as DOI: 10.1124/jpet.124.002238
This article has not been copyedited and formatted. The final version may differ from this version.

membranes were then incubated with IRDye 800 cw goat anti-rabbit secondary antibody at 1:100,00 dilution for 1 hour at room temperature. The membranes were developed and imaged using the Li-Cor Odyssey CLx imaging system. NIH image J was used for densitometry analysis.

11.Statistical Analysis: The data is expressed as means ± SE and analyzed using one-way ANOVA with Bonferroni correction for multiple group comparisons. Statistics were performed using GraphPad Prism 10 software (GraphPad Software, San Diego, CA), $p < 0.05$ was considered to be significant.

RESULTS

1. **Blockade of PI3K and p38 pathways abolish Irisin-induced improvement in hemodynamic in hemorrhage/resuscitation:** As shown in **Figures 2A & B**, we observed that prior to hemorrhage/resuscitation, the baseline MAP was comparable across all groups. Upon resuscitation, MAP recovered in each treatment group with varying degrees of improvement (**Fig. 2A & C**). Treatment of hemorrhage with irisin (Hemo + Irisin) demonstrated a significant increase in MAP compared to non-irisin groups, almost returning to baseline levels (**Fig. 2C**). However, the improvement in MAP of irisin was abrogated by Ly294002, an inhibitor of PI3K, and SB202190, an inhibitor of p38, although the MAP in irisin-treated groups did not significantly differ from hemorrhage control groups. Following resuscitation, a marked improvement in MAP was demonstrated by irisin infusion compared to other treatments (**Fig. 2D**). Notably, the reduction in MAP was observed in groups treated with either Ly294002 or SB202190 (**Fig. 2A & D**). Thus, these findings suggest that irisin treatment enhances hemodynamic stability after hemorrhage/resuscitation, which is inhibited by Ly294002 or SB202190.

JPET Fast Forward. Published on October 8, 2024 as DOI: 10.1124/jpet.124.002238
This article has not been copyedited and formatted. The final version may differ from this version.

2.Inhibition of PI3K and p38 pathways mitigated the improvement in cardiac function by irisin in Hemorrhage/Resuscitation: We have previously indicated that hemorrhage induced cardiac dysfunction assessed using echocardiography. In addition, irisin improved cardiac function and attenuated the detrimental effects of hemorrhage (Kulthinee S et al., 2022). Cardiac dysfunction in hemorrhage could lead to hypotension and hypoperfusion in organs to accelerate multiorgan dysfunction (Torres Filho, 2017). In this study, we extend our investigation to whether the effects of irisin on cardiac function in hemorrhage could be affected by the inhibition of PI3K and p38. As shown in **Table 1,** ejection fraction (EF) and fractional shortening (FS) were notably enhanced in groups treated with irisin (Hemo + Irisin) compared to control groups (Hemo + PBS). However, the cardiac protection of irisin post-hemorrhage/resuscitation was mitigated when irisin was co-infused with Ly294002 or SB202190. There was an increase in heart rate (HR) in Hemo/IR/P38i compared to Hemo/IR group. As shown in **Table 1**, irisin treatment showed a decrease in LVIDs in response to hemorrhage, which was abrogated by SB202190 or Ly294002. In addition, as compared to hemorrhage, irisin treatment showed a slight increase in IVS and LVPW, which disappeared by Ly294002 or SB202190. We noticed that irisin mitigated an increase in end-systolic volume (ESV), which also vanished by the treatment of SB202190 or Ly294002. **Figure 3** shows representative M-mode images of the LV post-hemorrhage/resuscitation among different groups. Therefore, irisin significantly enhanced ventricular function recovery after hemorrhage/resuscitation, which was abolished by the administration of Ly294002 or SB202190.

3. Inhibition of PI3K and p38 abrogated the impacts of irisin on attenuating inflammatory cytokines in hemorrhage/resuscitation: The release of inflammatory cytokines following hemorrhage acts as a critical factor leading to global ischemia-reperfusion injury (Zhang et al., 2010;

JPET Fast Forward. Published on October 8, 2024 as DOI: 10.1124/jpet.124.002238
This article has not been copyedited and formatted. The final version may differ from this version.

Cannon, 2018). We measured serum cytokines, including IL-6, TNF-α, and IL-1. As shown in (**Figure 4A-C)**, serum concentrations of these cytokines in the hemorrhage control were substantially mitigated by irisin treatment. However, when Ly294002 or SB202190 were administered, the effect of irisin on the suppression of cytokine levels in the hemorrhage disappeared.

4. Inhibition of PI3K and p38 attenuates the effect of irisin in reducing tissue damage in myocardium and skeletal muscle: As shown in **Figures 5A & C**, hemorrhage demonstrated an infiltration of substantial inflammatory cells in both myocardium and skeletal muscles. Notably, irisin treatment markedly reduced this infiltration in myocardium in hemorrhage. However, this reduction in tissue injury by irisin treatment was negated upon the administration of Ly294002 or SB202190. As shown in (**Figures 5B & D)**, the tissue injury scores in myocardium and skeletal muscle were significantly lower in the irisin-treated group. This decrease in injury scores by irisin was abrogated by Ly294002 and SB202190. Additionally, Ly6G positive neutrophile accumulations were significantly reduced by irisin treatment in both myocardium and skeletal muscles in hemorrhage. However, Ly294002 and SB202190 treatments abrogated the effects of irisin on the reduction of Ly6G positive neutrophile accumulations in both myocardium and skeletal muscles in hemorrhage (**data not shown**).

5. Inhibition of PI3K and p38 diminish anti-apoptosis of recombinant in myocardium and skeletal Muscles: Apoptosis of post-hemorrhage/resuscitation plays a critical role in determining the outcomes of trauma (Sharma et al., 2005). We conducted TUNEL staining in the myocardium and skeletal muscles. **Figures 6A&B** show that TUNEL-positive staining manifested in the myocardium in response to hemorrhage. However, irisin treatment markedly decreased the number of

JPET Fast Forward. Published on October 8, 2024 as DOI: 10.1124/jpet.124.002238
This article has not been copyedited and formatted. The final version may differ from this version.

TUNEL-positive signals, whereas Ly294002 or SB202190 abolished the effects of Irisin in reducing TUNEL positive signals. Likewise, irisin treatment resulted in a notable reduction in TUNEL-positive signals in skeletal muscles (**Figure 6C&D**). However, the functions of irisin on mitigating TUNEL positive staining in skeletal muscles were also attenuated by Ly294002 or SB202190.

6. Irisin enhances the phosphorylation of PI3K and p38 MAPK. We measured the activity of PI3K by measurement of phosphorylation of PI3K 85 subunit and phosphorylation of p38 in both skeletal and cardiac muscles. As shown in **Figure 7**, as compared to the hemorrhagic group, recombinant irisin treatment resulted in the recovery of both phosphorylation of PI3K 85 at Tyr 485/ Tyr 199 (**Figures 7 A, C, E and G**) and p38 at Thr182/Tyr180 (**Figure 7 B, D, F and H**) in both skeletal and cardiac muscle. However, the treatment of Ly294002 or SB202190 caused a marked reduction in both the phosphorylation of PI3K 85 and p38. Densitometric analysis indicated that the levels of phosphorylation of PI3K 85 (**Figures 7 C, G**) and p38 (**Figures 7 D, H**) were significantly attenuated by Ly294002 treatment or SB20219.

7. Inhibition of PI3K and p38 MAPK mitigated the effects of Irisin on expression of inflammatory cytokines in hemorrhage: Hemorrhage group showed an abundant expression of cytokines with regard to TNF-α (**Figure 8 B&D**) and IL1 (**Figure 8A&C**) in both skeletal muscle and cardiac muscle, which was significantly suppressed by the infusion of irisin. However, the effect of irisin in reducing muscle TNF-α and IL1 was diminished by the inhibition of either Ly294002 or SB20219, suggesting the effect of Irisin suppressing the expression of muscles TNF-α and IL1 is dependent on PI3K and p38 during hemorrhage/resuscitation.

JPET Fast Forward. Published on October 8, 2024 as DOI: 10.1124/jpet.124.002238
This article has not been copyedited and formatted. The final version may differ from this version.

DISCUSSION

Salient findings: To our knowledge, this is the first study to show that the protection of irisin treatment during hemorrhage/resuscitation are mediated through the PI3 kinase and p38 pathways. In this study, we have demonstrated that: **1)** Blockade of PI3K and p38 abrogated the improvements in cardiac performance and hemodynamics in hemorrhagic shock; **2)** The suppression of inflammatory cytokine-induced by irisin in hemorrhagic shock was mitigated by the inhibition of PI3K and p38; **3)** Blockade of PI3K and p38 abolished the anti-inflammatory cell infiltration and apoptosis induced by irisin against hemorrhage; **4)** Irisin alleviated the reduction of phosphorylated PI3K and phosphorylated p38 in the heart and muscles of hemorrhage, which were attenuated by the inhibition of PI3K and p38 pathway; **5)** Reduction of expression of inflammatory cytokines induced by irisin in hemorrhage was absent by inhibiting PI3K and p38 pathway. Overall, our findings provide a critical signaling pathway that PI3 kinase and p38 pathways mediate the protective effect of irisin against hemorrhagic injuries during hemorrhage/resuscitation.

Irisin, a cleaved fragment of the FNDC5 transmembrane precursor protein, predominantly found in muscles, the heart, and the brain, is known to be released during physical exercise. (Huh et al., 2012; Polyzos et al., 2013; Wrann et al., 2013). Increasing evidence suggests irisin's protective role during sepsis and ischemic cardiomyopathy (Matsuo et al., 2015; Ouyang et al., 2020; Pan et al., 2021). Our prior research indicated that irisin pre-treatment mitigated hypoxia/reoxygenation injury in cardiomyocytes (Zhao et al., 2016) and alleviated the detrimental effects of hemorrhagic shock, enhancing cardiac performance, augmenting insulin sensitivity, and reducing inflammatory response and damages in the lungs and muscles (Kulthinee et al., 2022). This study further confirms that irisin treatment improves hemodynamic stability, enhances cardiac function, and suppresses inflammatory

JPET Fast Forward. Published on October 8, 2024 as DOI: 10.1124/jpet.124.002238
This article has not been copyedited and formatted. The final version may differ from this version.

cytokine release following hemorrhage resuscitation (Wang et al., 2023b).

The PI3K signaling pathway serves as a critical mediator of cell proliferation, apoptosis inhibition, and inflammation (Shi et al., 2019). Activation of PI3K/Akt signaling reduced inflammatory responses and autophagy in ischemia-reperfusion injury (Yang et al., 2022; Zhou et al., 2023). It was reported that that PI3K pathways are closely associated with the functionality of irisin in the modulation of inflammatory and insulin sensitivity (Rabiee et al., 2020; Luna-Ceron et al., 2022; Zheng et al., 2022; Liu et al., 2023). Our recent work has demonstrated that irisin operates through multiple intracellular pathways, including AMPK (Yano et al., 2020; Wang et al., 2023b). Inhibition of the PI3K/Akt pathway exacerbates skeletal muscle ischemia-reperfusion injury in FNDC5 deficient mice, a precursor of irisin (Zhou et al., 2024). Our results revealed that hemorrhagic insults resulted in attenuation of phosphorylation of p85, a PI3K subunit, which was rescued by giving irisin, manifesting a role of irisin in activating PI3K in hemorrhagic shock. Pharmacologic inhibition of PI3K completely abrogated the protective effects of irisin in hemorrhage/resuscitation, indicating that PI3K contributes critically to the protective role induced by irisin. This is parallel with studies that irisin induced protective effects through attenuating inflammatory responses (Trettel et al 2023). Blockade of PI3K manifested the profound reduction in mean blood pressure in our study, suggesting that PI3K could be a key pathway to mediate vascular function in controlling mean blood pressure during hemorrhage. We have noticed that the blockade of PI3K abrogated the effects of irisin on the suppression of systemic inflammatory cytokines that contribute critically to the development of organ dysfunction (Li and Alam, 2011; Tsai et al., 2013; Niesler et al., 2014; Bonanno, 2020). Thus, the increased inflammatory cytokines by the inhibition of PI3K could be crucial in mitigating the recovery of cardiac functions generated by irisin in

JPET Fast Forward. Published on October 8, 2024 as DOI: 10.1124/jpet.124.002238
This article has not been copyedited and formatted. The final version may differ from this version.

hemorrhage.

Our previous work has demonstrated that irisin treatment enhances p38 phosphorylation in the myocardium, contributing to cardiac protection in ischemia-reperfusion injury (Wang et al., 2017). We found that both the deletion of PRAK, a p38 activator and high glucose reduce phosphorylated PI3 kinase, whereas irisin can preserve it (Zhang et al., 2021a). It was reported that irisin upregulates uncoupling protein-1 expression via p38 MAPK phosphorylation, stimulating white adipose tissue browning-specific genes in preventing obesity and associated type 2 diabetes (Zhang et al., 2014). p38 is crucial in signal transduction from cell surface receptors and are linked to prolonged cardiac protection in ischemic hearts (Rose et al., 2010, Zhao et al., 2001a; Zhao et al., 2001b). Previous studies have shown that the activation of p38 was involved in the regulation of hemorrhagic injury, but showed conflicting results, which is likely related to different models, and the magnitude of p38 activation (Hsu et al., 2008; Kan et al., 2008; Liu et al., 2012; Lv et al., 2012). While previous studies indicated that p38 serves as a key signal in association with irisin to modulate insulin sensitivity (Sanchis-Gomar and Perez-Quilis, 2014; Zhang et al., 2014; Lee et al., 2015), in this study, we observed that the administration of a p38 inhibitor diminished irisin's protective effects in hemorrhage. In agreement with our studies, it was reported that irisin treatment increases the level of phosphorylated-p38 during ischemia/reperfusion (Askari H et al 2018*)*. However, other studies found that irisin inhibits osteoblast apoptosis by inhibiting the p38 MAPK to target chondrocytes and stimulate cellular anabolism and attenuate catabolism, thereby suppressing osteoarthritis progression (Zhao R et al., 2023). It was also reported that blocking p38 MAPK mitigates the development of the renal dysfunction in hemorrhagic shock (Sato et al., 2005). The difference in these studies is not clear, but likely stems from the different models employed in these studies. In addition, previous report

JPET Fast Forward. Published on October 8, 2024 as DOI: 10.1124/jpet.124.002238
This article has not been copyedited and formatted. The final version may differ from this version.

indicates that the genetic deletion of p38 illustrated detrimental effects without affecting heart rate, but we have noticed that the inhibition of p38 in hemorrhage showed an increase in heart rate in this study. The reason for an increase in HR following p38 inhibitor in this model is not clear, which merits further investigation in future studies. Our studies also indicate that the inhibition of inflammatory responses contributes critically to the protection of irisin against hemorrhage/resuscitation. In addition to mitigating inflammatory cell infiltration, the suppression of Ly6G positive neutrophile infiltration by irisin in cardiac and skeletal muscles accounts for the role of irisin in attenuating inflammatory responses via PI3K and p38 in hemorrhage (Carai P et al, 2023; Kain V et al 2019). However, it is not clear whether other specific populations of inflammation cells such as macrophages etc. will also be affected by irisin/PI3K and p38 in modulation of inflammation in hemorrhage. Our studies have indicated that both PI3K and P38 are engaged in the generation of the protective effect of irisin during hemorrhage/resuscitation. However, we could not identify whether PI3K and p38 individually or synchronizes to modulate the effect of irisin against hemorrhage. It is not clear whether PI3K and p38 could form a cascade to modulate the functionality of irisin in the event of hemorrhage/resuscitation, which is interesting and needs further investigation. In this study, DMSO was used vehicle for dissolvents of PI3K and p38 inhibitors in either hemorrhage or hemorrhage treated with irisin. There was no significant effect on cardiac function between DMSO and dissolvent of irisin (PBS). This allowed for the combination of PBS and DMSO treatments in either hemorrhage or hemorrhage treated with irisin, which increases the sample size of control and improves the rigor in this study to define the role of this pathway on hemorrhage.

In conclusion, our study has established that irisin provides protective effects in hemorrhage/resuscitation. This is evidenced by improved hemodynamic stability, enhanced cardiac

function, and a decrease in inflammatory cytokine release, histological damage, and cell apoptosis. Notably, these beneficial effects of irisin are negated when the PI3 kinase and p38 pathways are inhibited. Collectively, our findings suggest that irisin/PI3K and irisin/p38 are crucial pathways for mitigating hemorrhage/resuscitation injury, which offers a promising avenue for new therapeutic strategies in managing hemorrhage/resuscitation.

Data Availability Statement: The authors declare that all the data supporting the findings of this study are contained within this manuscript.

Authorship Contributions:

Participated in research design: Wen, Yano, T.C. Zhao.

Conducted experiments: Wen, T.C. Zhao, Wei, T. Zhao.

Performed data analysis: Wen, Yano, T.C. Zhao.

Wrote or contributed to the editing of the manuscript: Wen, T. Zhao, Yano, Wei, T.C. Zhao

REFERENCES

Almeida González D, Rodríguez-Pérez MDC, Fuentes Ferrer M, Cuevas Fernández FJ, Marcelino Rodríguez I, Cabrera de León A. Irisin (2023) in women and men: blood pressure, heart rate, obesity and insulin resistance. *Front Endocrinol (Lausanne)* 14:1193110.

Alves HR, Lomba GSB, Gonçalves-de-Albuquerque CF, Burth P (2022) Irisin, exercise, and COVID-19. *Front Endocrinol (Lausanne)* 13:879066.

Andaluz N and Zuccarello M (2009) Recent trends in the treatment of spontaneous intracerebral hemorrhage: analysis of a nationwide inpatient database. *J Neurosurg* **110**:403-410.

Askari H, Rajani SF, Poorebrahim M, Haghi-Aminjan H, Raeis-Abdollahi E and Abdollahi M (2018) A glance at the therapeutic potential of irisin against diseases involving inflammation, oxidative stress, and apoptosis: An introductory review. *Pharmacological research*

129:44-55.

Bonanno FG (2020) The Need for a Physiological Classification of Hemorrhagic Shock. *J Emerg Trauma Shock* **13**:177-182.

Bostrom P, Wu J, Jedrychowski MP, Korde A, Ye L, Lo JC, Rasbach KA, Bostrom EA, Choi JH, Long JZ, Kajimura S, Zingaretti MC, Vind BF, Tu H, Cinti S, Hojlund K, Gygi SP and Spiegelman BM (2012) A PGC1-alpha-dependent myokine that drives brown-fat-like development of white fat and thermogenesis. *Nature* **481**:463-468.

Cai Z and Semenza GL (2004) Phosphatidylinositol-3-kinase signaling is required for erythropoietin-mediated acute protection against myocardial ischemia/reperfusion injury. *Circulation* **109**:2050-2053.

Carai P, González LF, Van Bruggen S, Spalart V, De Giorgio D, Geuens N, Martinod K, Jones EAV, Heymans S (2023) Neutrophil inhibition improves acute inflammation in a murine model of viral myocarditis. *Cardiovasc Res* 118(17):3331-3345

Cannon JW (2018) Hemorrhagic Shock. *The New England journal of medicine* **378**:370-379.

Cantley LC (2002) The phosphoinositide 3-kinase pathway. *Science* **296**:1655-1657.

Deniau B, Ricbourg A, Weiss E, Paugam-Burtz C, Bonnet MP, Goffinet F, Mignon A, Morel O, Le Guen M, Binczak M, Carbonnel M, Michelet D, Dahmani S, Pili-Floury S, Ducloy Bouthors AS, Mebazaa A, Gayat E (2024). Association of severe postpartum hemorrhage and development of psychological disorders: Results from the prospective and multicentre HELP MOM study. *Anaesth Crit Care Pain Med* 43(2):101340.

Durrant TN and Hers I (2020) PI3K inhibitors in thrombosis and cardiovascular disease. *Clinical and translational medicine* **9**:8.

El Ayadi A, Raifman S, Jega F, Butrick E, Ojo Y, Geller S and Miller S (2013) Comorbidities and lack of blood transfusion may negatively affect maternal outcomes of women with obstetric hemorrhage treated with NASG. *PloS one* **8**:e70446.

Gruen RL, Brohi K, Schreiber M, Balogh ZJ, Pitt V, Narayan M and Maier RV (2012) Haemorrhage control in severely injured patients. *Lancet (London, England)* **380**:1099-1108.

Gutierrez G, Reines HD, Wulf-Gutierrez ME (2004) Clinical review: hemorrhagic shock. *Crit Care* 8(5):373-81.

Han F, Ding ZF, Shi XL, Zhu QT, Shen QH, Xu XM, Zhang JX, Gong WJ, Xiao WM, Wang D, Chen WW, Hu LH and Lu GT (2023) Irisin inhibits neutrophil extracellular traps formation and protects against acute pancreatitis in mice. *Redox biology* **64**:102787.

Hsu JT, Kan WH, Hsieh CH, Choudhry MA, Schwacha MG, Bland KI and Chaudry IH (2008) Mechanism of estrogen-mediated intestinal protection following trauma-hemorrhage: p38 MAPK-dependent upregulation of HO-1. *Am J Physiol Regul Integr Comp Physiol* **294**:R1825-1831.

Huang X, Xiao J, Wang X and Cao Z (2022) Irisin attenuates P. gingivalis-suppressed osteogenic/cementogenic differentiation of periodontal ligament cells via p38 signaling pathway. *Biochemical and biophysical research communications* **618**:100-106.

Huh JY, Panagiotou G, Mougios V, Brinkoetter M, Vamvini MT, Schneider BE and Mantzoros CS (2012) FNDC5 and irisin in humans: I. Predictors of circulating concentrations in serum and plasma and II. mRNA expression and circulating concentrations in response to weight loss and exercise. *Metabolism: clinical and experimental* **61**:1725-1738.

Hwabejire JO, Lu J, Liu B, Li Y, Halaweish I, Alam HB (2014) Valproic acid for the treatment of hemorrhagic shock: a dose-optimization study. *J Surg Res* 186(1):363-70.

Jarrar D, Chaudry IH and Wang P (1999) Organ dysfunction following hemorrhage and sepsis: mechanisms and therapeutic approaches (Review). *Int J Mol Med* **4**:575-583.

Jedrychowski MP, Wrann CD, Paulo JA, Gerber KK, Szpyt J, Robinson MM, Nair KS, Gygi SP and Spiegelman BM (2015) Detection and quantitation of circulating human Irisin by tandem mass spectrometry. *Cell Metab* **22**:734-740.

Kan WH, Hsu JT, Ba ZF, Schwacha MG, Chen J, Choudhry MA, Bland KI and Chaudry IH (2008) p38 MAPK-dependent eNOS upregulation is critical for 17beta-estradiol-mediated cardioprotection following trauma-hemorrhage. *American journal of physiology Heart and circulatory physiology* **294**:H2627-2636.

Kain V, Jadapalli JK, Tourki B, Halade GV (2019) Inhibition of FPR2 impaired leukocytes recruitment and elicited non-resolving inflammation in acute heart failure. *Pharmacol Res*146:104295.

Tang WK, Wang L, F Tsoi KK, Kim JS (2023). Post-Traumatic Stress Disorder after Subarachnoid

Hemorrhage: A Systematic Review. *Neurol India* 71(1):9-19.

Kulthinee S, Wang L, Yano N, Dubielecka PM, Zhang LX, Zhuang S, Qin G, Zhao YT, Eugene Chin Y and Zhao TC (2022) Irisin preserves cardiac performance and insulin sensitivity in response to hemorrhage. *Pharmaceuticals (Basel)* **15**.

Lee HJ, Lee JO, Kim N, Kim JK, Kim HI, Lee YW, Kim SJ, Choi JI, Oh Y, Kim JH, Suyeon H, Park SH and Kim HS (2015) Irisin, a novel myokine, regulates glucose uptake in skeletal muscle cells via AMPK. *Molecular endocrinology (Baltimore, Md)* **29**:873-881.

Li Y and Alam HB (2011) Modulation of acetylation: creating a pro-survival and anti-inflammatory phenotype in lethal hemorrhagic and septic shock. *J Biomed Biotechnol* **2011**:523481.

Liu C, Wei A, Wang T (2022) Irisin, an effective treatment for cardiovascular diseases? J Cardiovasc *Dev Dis* 9(9):305.

Liu FC, Hwang TL, Liu FW, Yu HP (2012) Tropisetron attenuates cardiac injury in a rat trauma-hemorrhage model. *Shock*38(1):76-81.

Liu FC, Liu FW, Yu HP (2010) Ondansetron attenuates hepatic injury via p38 MAPK-dependent pathway in a rat haemorrhagic shock model. *Resuscitation* 82(3):335-40.

Liu FC, Yu HP, Hwang TL and Tsai YF (2012) Protective effect of tropisetron on rodent hepatic injury after trauma-hemorrhagic shock through P38 MAPK-dependent hemeoxygenase-1 expression. *PloS one* **7**:e53203.

Liu JF, Su G, Chen LX, Zhou JP, Gao J, Zhang JJ, Wu QH, Chen W, Chen DY and Zhang ZC (2023) Irisin attenuates apoptosis following ischemia-reperfusion injury through improved mitochondria dynamics and ROS suppression mediated through the PI3K/Akt/mTOR axis. *Mol Neurobiol* **60**:4261-4272.

Liu S, Cui F, Ning K, Wang Z, Fu P, Wang D, Xu H (2022) Role of irisin in physiology and pathology. *Front Endocrinol (Lausanne).* 202213:962968.

Luna-Ceron E, Gonzalez-Gil AM and Elizondo-Montemayor L (2022). Current insights on the role of Irisin in endothelial dysfunction. *Curr Vasc Pharmacol* **20**:205-220.

Luo Y, Qiao X, Ma Y, Deng H, Xu CC,Xu L (2020) Disordered metabolism in mice lacking irisin. *Sci Rep* 2020;10(1):17368.

Lv KY, Yu XY, Bai YS, Zhu SH, Tang HT, Ben DF, Xiao SC, Wang GY, Ma B and Xia ZF (2012)

Role of inhibition of p38 mitogen-activated protein kinase in liver dysfunction after hemorrhagic shock and resuscitation. *J Surg Res* **178**:827-832.

Matsuo Y, Gleitsmann K, Mangner N, Werner S, Fischer T, Bowen TS, Kricke A, Matsumoto Y, Kurabayashi M, Schuler G, Linke A and Adams V (2015) Fibronectin type III domain containing 5 expression in skeletal muscle in chronic heart failure-relevance of inflammatory cytokines. *Journal of cachexia, sarcopenia and muscle* **6**:62-72.

Mazur-Bialy AI, Pocheć E and Zarawski M (2017) Anti-inflammatory properties of irisin, mediator of physical activity, are connected with TLR4/MyD88 signaling pathway activation. *International journal of molecular sciences* **18**.

Mińko A, Turoń-Skrzypińska A, Rył A, Mańkowska K, Cymbaluk-Płoska A, Rotter I (2024) The significance of selected myokines in predicting thelength of rehabilitation of patients after COVID-19 infection. *Biomedicines* 12(4):836.

Niesler U, Palmer A, Radermacher P and Huber-Lang MS (2014) Role of alveolar macrophages in the inflammatory response after trauma. *Shock (Augusta, Ga)* **42**:3-10.

Nishida K, Yamaguchi O, Hirotani S, Hikoso S, Higuchi Y, Watanabe T, Takeda T, Osuka S, Morita T, Kondoh G, Uno Y, Kashiwase K, Taniike M, Nakai A, Matsumura Y, Miyazaki J, Sudo T, Hongo K, Kusakari Y, Kurihara S, Chien KR, Takeda J, Hori M, Otsu K (2004). p38alpha mitogen-activated protein kinase plays a critical role in cardiomyocyte survival but not in cardiac hypertrophic growth in response to pressure overload. *Mol Cell Biol* 24(24):10611-20.

Ouyang H, Li Q, Zhong J, Xia F, Zheng S, Lu J, Deng Y and Hu Y (2020) Combination of melatonin and irisin ameliorates lipopolysaccharide-induced cardiac dysfunction through suppressing the Mst1-JNK pathways. *Journal of cellular physiology* **235**:6647-6659.

Pan JA, Zhang H, Yu Q, Zhang JF, Wang CQ, Gu J and Chen K (2021) Association of circulating Irisin levels and the characteristics and prognosis of coronary artery disease. *Am J Med Sci* **362**:63-71.

Polyzos SA, Kountouras J, Shields K and Mantzoros CS (2013) Irisin: a renaissance in metabolism? *Metabolism: clinical and experimental* **62**:1037-1044.

Rabiee F, Lachinani L, Ghaedi S, Nasr-Esfahani MH, Megraw TL and Ghaedi K (2020) New insights

into the cellular activities of Fndc5/Irisin and its signaling pathways. *Cell & bioscience* **10**:51.

Rana KS, Pararasa C, Afzal I, Nagel DA, Hill EJ, Bailey CJ, Griffiths HR, Kyrou I, Randeva HS, Bellary S, Brown JE (2017) Plasma irisin is elevated in type 2 diabetes and is associated with increased E-selectin levels. *Cardiovasc Diabetol* 16(1):147.

Rose BA, Force T and Wang Y (2010) Mitogen-activated protein kinase signaling in the heart: angels versus demons in a heart-breaking tale. *Physiological reviews* **90**:1507-1546.

Roux PP and Blenis J (2004) ERK and p38 MAPK-activated protein kinases: a family of protein kinases with diverse biological functions. *Microbiol Mol Biol Rev* **68**:320-344.

Sanchis-Gomar F and Perez-Quilis C (2014) The p38-PGC-1α-irisin-betatrophin axis: Exploring new pathways in insulin resistance. *Adipocyte* **3**:67-68.

Sato H, Tanaka T, Kasai K, Kita T, Tanaka N (2005) Role of p38 mitogen-activated protein kinase on renal dysfunction after hemorrhagic shock in rats. *Shock* 24(5):488-94.

Sharma P, Walsh KT, Kerr-Knott KA, Karaian JE and Mongan PD (2005) Pyruvate modulates hepatic mitochondrial functions and reduces apoptosis indicators during hemorrhagic shock in rats. *Anesthesiology* **103**:65-73.

Shi X, Wang J, Lei Y, Cong C, Tan D and Zhou X (2019) Research progress on the PI3K/AKT signaling pathway in gynecological cancer (Review). *Mol Med Rep* **19**:4529-4535.

Shoko T, Shiraishi A, Kaji M and Otomo Y (2010) Effect of pre-existing medical conditions on in-hospital mortality: analysis of 20,257 trauma patients in Japan. *J Am Coll Surg* **211**:338-346.

Simpson R, Praditsuktavorn B, Wall J, Morales V, Thiemermann C, Tremoleda JL, Brohi K (2023) Myocardial alterations following traumatic hemorrhagic injury. *J Trauma Acute Care Surg* 95(4):481-489.

Torres Filho I (2017). Hemorrhagic Shock and the Microvasculature. Compr Physiol 8(1):61-101.

Trettel CDS, Pelozin BRA, Barros MP, Bachi ALL, Braga PGS, Momesso CM, Furtado GE, Valente PA, Oliveira EM, Hogervorst E, Fernandes T (2023) Irisin: An anti-inflammatory exerkine in aging and redox-mediated comorbidities. *Front Endocrinol (Lausanne)* 14:1106529

Tsai TT, Chuang YJ, Lin YS, Wan SW, Chen CL and Lin CF (2013) An emerging role for the

anti-inflammatory cytokine interleukin-10 in dengue virus infection. *Journal of biomedical science* **20**:40.

Tsai YF, Liu FC, Lau YT and Yu HP (2012) Role of Akt-dependent pathway in resveratrol-mediated cardioprotection after trauma-hemorrhage. *J Surg Res* **176**:171-177.

Wall J, Naganathar S, Praditsuktavorn B, Bugg OF, McArthur S, Thiemermann C, Tremoleda JL, Brohi K (2019) Modeling cardiac dysfunction following traumatic hemorrhage injury: Impact on myocardial integrity. *Front Immunol*10:2774.

Wang FS, Kuo CW, Ko JY, Chen YS, Wang SY, Ke HJ, Kuo PC, Lee CH, Wu JC, Lu WB, Tai MH, Jahr H and Lian WS (2020a) Irisin mitigates oxidative stress, chondrocyte dysfunction and osteoarthritis development through regulating mitochondrial integrity and autophagy. *Antioxidants (Basel)* **9**.

Wang H, Zhao YT, Zhang S, Dubielecka PM, Du J, Yano N, Chin YE, Zhuang S, Qin G and Zhao TC (2017) Irisin plays a pivotal role to protect the heart against ischemia and reperfusion injury. *Journal of cellular physiology* **232**:3775-3785.

Wang J, Zhao YT, Zhang L, Dubielecka PM, Qin G, Chin YE, Gower AC, Zhuang S, Liu PM and Zhao TC (2023a) Irisin deficiency exacerbates diet-induced insulin resistance and cardiac dysfunction in type II diabetes in mice. *American journal of physiology Cell physiology*.

Wang J, Zhao YT, Zhang L, Dubielecka PM, Zhuang S, Qin G, Chin YE, Zhang S and Zhao TC (2020b) Irisin improves myocardial performance and attenuates insulin resistance in spontaneous mutation (Lepr(db)) mice. *Frontiers in pharmacology* **11**:769.

Wang L, Kulthinee S, Slate-Romano J, Zhao T, Shanmugam H, Dubielecka PM, Zhang LX, Qin G, Zhuang S, Chin YE and Zhao TC (2023b) Inhibition of integrin alpha v/beta 5 mitigates the protective effect induced by irisin in hemorrhage. *Experimental and molecular pathology* **134**:104869.

Wang PW, Pang Q, Zhou T, Song XY, Pan YJ, Jia LP, Zhang AH (2022) Irisin alleviates vascular calcification by inhibiting VSMC osteoblastic transformation and mitochondria dysfunction via AMPK/Drp1 signaling pathway in chronic kidney disease. *Atherosclerosis* 346:36-45.

Wilson NM, Wall J, Naganathar V, Brohi K, De'Ath HD (2017) Mechanisms involved in secondary

cardiac dysfunction in animal models of trauma and hemorrhagic shock. *Shock* 48(4):401-410.

Wrann CD, White JP, Salogiannnis J, Laznik-Bogoslavski D, Wu J, Ma D, Lin JD, Greenberg ME and Spiegelman BM (2013) Exercise induces hippocampal BDNF through a PGC-1α/FNDC5 pathway. *Cell Metab* **18**:649-659.

Yang F, Chen ZR, Yang XH, Xu Y, Ran NJ, Liu MJ, Jin SG, Jia HN and Zhang Y (2022) Monomethyl lithospermate alleviates ischemic stroke injury in middle cerebral artery occlusion mice in vivo and protects oxygen glucose deprivation/reoxygenation induced SHSY-5Y cells in vitro via activation of PI3K/Akt signaling. *Frontiers in pharmacology* **13**:1024439.

Yano N, Zhang L, Wei D, Dubielecka PM, Wei L, Zhuang S, Zhu P, Qin G, Liu PY, Chin YE and Zhao TC (2020) Irisin counteracts high glucose and fatty acid-induced cytotoxicity by preserving the AMPK-insulin receptor signaling axis in C2C12 myoblasts. *American journal of physiology Endocrinology and metabolism* **318**:E791-e805.

Zhang L, Wang J, Zhao YT, Dubielecka P, Qin G, Zhuang S, Chin EY, Liu PY and Zhao TC (2021a) Deletion of PRAK mitigates the mitochondria function and suppresses insulin signaling in C2C12 myoblasts exposed to high glucose. *Frontiers in pharmacology* **12**:698714.

Zhang Q, Raoof M, Chen Y, Sumi Y, Sursal T, Junger W, Brohi K, Itagaki K and Hauser CJ (2010) Circulating mitochondrial DAMPs cause inflammatory responses to injury. *Nature* **464**:104-107.

Zhang Y, Li R, Meng Y, Li S, Donelan W, Zhao Y, Qi L, Zhang M, Wang X, Cui T, Yang LJ and Tang D (2014) Irisin stimulates browning of white adipocytes through mitogen-activated protein kinase p38 MAP kinase and ERK MAP kinase signaling. *Diabetes* **63**:514-525.

Zhao R, Chen Y, Wang D, Zhang C, Song H,Ni G (2023) Role of irisin in bone diseases. *Front Endocrinol (Lausanne)* 14:1212892.

Zhao TC, Cheng G, Zhang LX, Tseng YT and Padbury JF (2007) Inhibition of histone deacetylases triggers pharmacologic preconditioning effects against myocardial ischemic injury. *Cardiovascular research* **76**:473-481.

Zhao TC, Du J, Zhuang S, Liu P and Zhang LX (2013) HDAC inhibition elicits myocardial

protective effect through modulation of MKK3/Akt-1. *PloS one* **8**:e65474.

Zhao TC, Hines DS and Kukreja RC (2001a) Adenosine-induced late preconditioning in mouse hearts: role of p38 MAP kinase and mitochondrial K(ATP) channels. *American journal of physiology Heart and circulatory physiology* **280**:H1278-1285.

Zhao TC, Taher MM, Valerie KC and Kukreja RC (2001b) p38 Triggers late preconditioning elicited by anisomycin in heart: involvement of NF-kappaB and iNOS. *Circulation research* **89**:915-922.

Zhao YT, Wang H, Zhang S, Du J, Zhuang S and Zhao TC (2016) Irisin ameliorates hypoxia/reoxygenation-induced injury through modulation of histone deacetylase 4. *PloS one* **11**:e0166182.

Zheng S, Chen N, Kang X, Hu Y and Shi S (2022) Irisin alleviates FFA induced β-cell insulin resistance and inflammatory response through activating PI3K/AKT/FOXO1 signaling pathway. *Endocrine* **75**:740-751.

Zhou M, Wang K, Jin Y, Liu J, Wang Y, Xue Y, Liu H, Chen Q, Cao Z, Jia X and Rui Y (2024) Explore novel molecular mechanisms of FNDC5 in ischemia-reperfusion (I/R) injury by analyzing transcriptome changes in mouse model of skeletal muscle I/R injury with FNDC5 knockout. *Cell Signal* **113**:110959.

Zhou M, Zhang H, Chen H and Qi B (2023) Adiponectin protects skeletal muscle from ischaemia-reperfusion injury in mice through miR-21/PI3K/Akt signalling pathway. *International wound journal* **20**:1647-1661.

Footnotes. The work is supported by the National Institute of. General Medical Sciences (R01GM 141339) and the National Heart, Lung, and Blood Institute Grants (R01 HL089405). No author has an actual or perceived conflict of interest with the contents of this article.

Figure Legends:

Figure 1. The protocol of hemorrhage and resuscitation. Mice were maintained MAP at 35~45

JPET Fast Forward. Published on October 8, 2024 as DOI: 10.1124/jpet.124.002238
This article has not been copyedited and formatted. The final version may differ from this version.

mmHg for one hour. Following this, resuscitation was carried out using a volume three times that of the extracted blood, which included both the withdrawn blood and lactated Ringer's solution (LRS). The experimental protocol summarizes experimental groups/retreatment in hemorrhage/resuscitation and an assay of post-resuscitation and sample size.

Figure 2. Time-MAP course during the hemorrhage/resuscitation and the MAP in mice exposed to hemorrhage: **A**: The time-MAP course during the hemorrhage/resuscitation; **B**: The baseline MAP before hemorrhage; **C**: The MAP after completing resuscitation; **D**: The MAP after 1 hour of resuscitation; Hemo+PBS (n=12); Hemo+Irisin (n=13); Hemo+IR+ Ly294002 (n=6); Hemo+IR+ SB202190 (n=6). Data are shown as Mean ± SEM *p < 0.05; **p < 0.01; ***p < 0.001; ****p < 0.0001. F = 38.65 (**B**); 24.29 (**C**) and 0.52 (**D**) in ANOVA. Hemo, Hemorrhage; IR, irisin; PI3Ki, PI3 kinase inhibitor: Ly294002; p38i, p38 MAPK inhibitor: SB202190;

Figure 3. Representative images of LV with M mode in mice exposed to hemorrhage/resuscitation. Images of echocardiography was captured at two hours following hemorrhage and resuscitation. The scale on images: a speed at 75 mm/second; a depth of 1.5 cm. Hemo, Hemorrhage; IR, irisin; PI3Ki, PI3 kinase inhibitor: Ly294002; p38i, P38 MAPK inhibitor: SB202190.

Figure 4. ELISA analysis of IL-6, TNF-α, and IL-1 in serum. **A**: Levels of IL-6 in serum; **B**: Serum levels of TNF-α; **C**: Levels of IL-1 in serum. Data are shown as Mean ± SEM. Animal number in each group for heart and skeletal muscle tissue were as follows: Hemorrhage (8); Hemorrhage +irisin (n=8); hemorrhage+Irisin+Ly294002 (n=4); Hemorrhage+Irisin+SB202190 (n=4) for heart and skeletal muscles. ***p < 0.001; ****p < 0.0001 versus Hemo+Irisin; F=57.74 in (**A)**, 181.4 in (**B)** and 26.1 in (**C)** in ANOVA.

Figure 5. Histological analysis of pathological injury in skeletal muscle (GAS), and myocardium tissues. **A**: H&E staining showing inflammatory cell infiltration in myocardium (scale bars indicate 100 μm); **B**: A bar graph showing tissue injury index score in myocardium; ****p< 0.0001 versus

JPET Fast Forward. Published on October 8, 2024 as DOI: 10.1124/jpet.124.002238
This article has not been copyedited and formatted. The final version may differ from this version.

Hemo+Irisin; F=187.1 in ANOVA. **C**: H&E staining showing inflammatory cell infiltration in skeletal muscle (scale bars indicate 100 μm); **D**: A bar graph showing tissue injury index score in skeletal muscle; Data are shown as Mean ± SEM. ****p < 0.0001 versus Hemo+Irisin; F=36.9 in ANOVA; Hemorrhage (n=6); Hemorrhage +irisin (n=6); Hemorrhage+Irisin+Ly294002 (n=6); Hemorrhage+Irisin+SB202190 (n=6) for heart and skeletal muscles; Hemo, hemorrhage; PI3Ki, PI3 kinase inhibitor Ly294002; p38i, P38 MAPK inhibitors SB202190;

Figure 6. TUNEL staining of apoptosis in the myocardium and skeletal muscles (GAS) following hemorrhage/resuscitation. **A**: The image of TUNEL-positive nuclei in the myocardium (scale bar 100 μm); **B**: A bar graph for data of TUNEL-positive nuclei in the myocardium; Data are expressed as Mean ± SEM; F=47.6 in ANOVA; **C:** The image of TUNEL-positive nuclei in skeletal muscle (scale bar: 100 μm); **D**: A bar graph for data of TUNEL-positive nuclei in skeletal muscle; Data are expressed as Mean ± SEM; F=43.1 in ANOVA. Animal numbers in each group were as follows: Hemorrhage (n=6); Hemorrhage +irisin (n=6); hemorrhage+Irisin+Ly294002 (n=6); Hemorrhage+Irisin+SB202190 (n=6) for both heart and skeletal muscles. ****p < 0.0001 versus Hemo+Irisin. TUNLE positive nuclei were normalized to areas observed under microscope. Hemo, hemorrhage; PI3Ki, PI3 kinase inhibitor Ly294002; p38i, P38 MAPK inhibitors SB202190.

Figure 7. Western blot and densitometric analysis showing phosphorylated PI3K-p85 subunit, non-phosphorylated PI3K-p85 subunit, phosphorylated p38 and non-phosphorylated p38 in skeletal muscles (GAS) and cardiac muscles of mouse exposed to hemorrhage and resuscitation. **A-H**: Western blot and densitometric analysis showing phosphorylated PI3K-p85 subunit, non-phosphorylated PI3K-p85 subunit (**A, C**) in skeletal muscle and (**E, G**) in myocardium, phosphorylated p38 and non-phosphorylated p38 in skeletal (**B, D**) and cardiac muscle (**F, H**) of mouse exposed to hemorrhage/resuscitation. Values represent means ± SE. Animal numbers in each group were as follows: Hemorrhage (n=6); Hemorrhage +irisin (n=6); hemorrhage+Irisin+Ly294002 (n=6); Hemorrhage+Irisin+SB202190 (n=6) for heart and skeletal muscles. ***p < 0.001; ****p < 0.0001 versus Hemo+Irisin. Results are expressed as fold increase of hemorrhage in **C, D, G and H**. F= 31.73 (**C**), 90.78 (**D**), 15.14 (**G**) and 121.7(**H**) in ANOVA. Hemo, hemorrhage; PI3Ki, PI3 kinase

JPET Fast Forward. Published on October 8, 2024 as DOI: 10.1124/jpet.124.002238
This article has not been copyedited and formatted. The final version may differ from this version.

inhibitor Ly294002; p38i, P38 MAPK inhibitors SB202190.

Figure 8. qPCR confirmed the transcriptional change in inflammatory cytokine including IL1 mRNA and TNF-α mRNA in cardiac muscle (**A, B**) and skeletal muscles (GAS) (**C, D**) of mice exposed to hemorrhage/resuscitation. Animal numbers in each group were as follows: Hemorrhage (n=8); Hemorrhage +irisin (n=8); hemorrhage+Irisin+Ly294002 (n=5); Hemorrhage+Irisin+SB202190 (n=5) for heart and skeletal muscles. Values represent means ± SE. ****p<0.0001 versus Hemo+Irisin. F=76.75 (**A**); 142.6 (**B**); 125.3(**C**) and 53.8 (**D**) in ANOVA. Hemo, hemorrhage; PI3Ki, PI3 kinase inhibitor: Ly294002; p38i, P38 MAPK inhibitor: SB202190.

Table 1: Echocardiographic Parameters in hemorrhage/resuscitation

Groups Parameters	Hemo+PBS (n = 13)	Hemo+IR (n = 12)	Hemo+IR+PI3Ki (n = 6)	Hemo+IR+p38i (n = 6)	F value
HR (BPM)	496±9	475±15	516±31	540±12*	3.33
EF (%)	59.8±1.11****	72.3+0.46	55.0±1.45****	54.8±1.66****	130.3
FS (%)	26.2±0.58****	34.8±0.37	23.3±0.76****	23.0±0.71****	148.0
IVSd (MM)	0.64±0.02	0.73±0.05	0.58±0.02*	0.56±0.02*	4.48

JPET Fast Forward. Published on October 8, 2024 as DOI: 10.1124/jpet.124.002238
This article has not been copyedited and formatted. The final version may differ from this version.

IVSs (MM)	0.64±0.04	0.79±0.05	0.65±0.04	0.58±0.04*	3.74
LVIDd (MM)	4.33±0.09**	3.78±0.14	4.15±0.16	4.48±0.14**	6.39
LVIDs (MM)	3.19±0.07****	2.32±0.17	3.21±0.11***	3.52±0.10****	18.37
LVPWd (MM)	0.85±0.03	0.94±0.04	0.76±0.04*	0.78±0.05	4.23
LVPWs (MM)	1.00±0.05	1.13±0.03	0.78±0.07***	0.88±0.09*	8.29
LVvold/EDV (ml)	0.08±0.00**	0.06±0.00	0.07±0.01	0.09±0.01**	7.42
LVvols/ESV (ml)	0.03±0.00****	0.02±0.00	0.03±0.00***	0.04±0.00****	21.07

Abbreviations in Table 1 are described in the section of abbreviations in main text: Results are expressed as Mean ± SEM (n = 6~13/per group). $^{*}p < 0.05$; $^{**}p< 0.01$; $^{***}p < 0.001$; $^{****}p < 0.0001$. All comparisons in the table are between the other three groups and the 'Hemo+IR' group. Hemo, Hemorrhage; IR, irisin; PI3Ki, PI3 kinase inhibitor Ly294002; p38i, P38 MAPK inhibitors

Figure1

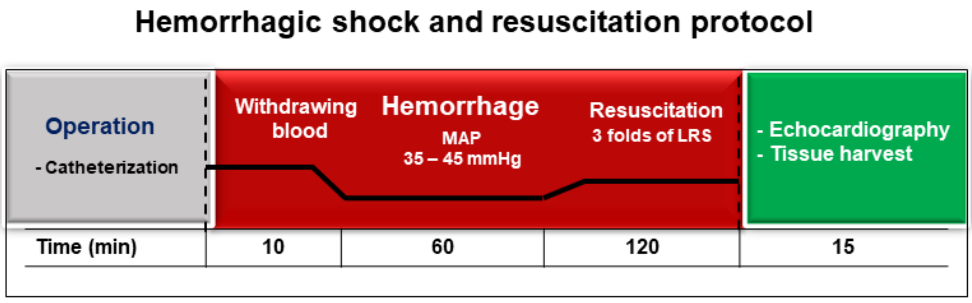

Experimental groups in H/R, Treatments & drug doses

Hemo+PBS:
PBS only

Hemo+Irisin:
(irisin 5μ g/kg, i.v)

Hemo+Irisin+Ly294002:
(Irisin, 5μ g/kg; Ly294002, 1mg/kg, i.v.)

Hemo+Irisin+ SB202190
(irisin 5μ g/kg, SB202190 1mg/kg, i.v)

Resuscitation

At onset of R

Assay of Post-Resuscitation and sample size

- **Echocardiography (n= 6-13 /per group)**
- **Serum cytokine by ELISA (n=4-8/per group)**
- **Histological analysis of tissue injury in heart & muscles (n=6/per group)**
- **TUNEL analysis in heart & muscles (n=6/per group)**
- **Cytokine genes in heart & muscles (n=5-8/ per group)**
- **Immunoblot of p38 and PI3K in heart & muscles(n=6/per group)**

Figure 2

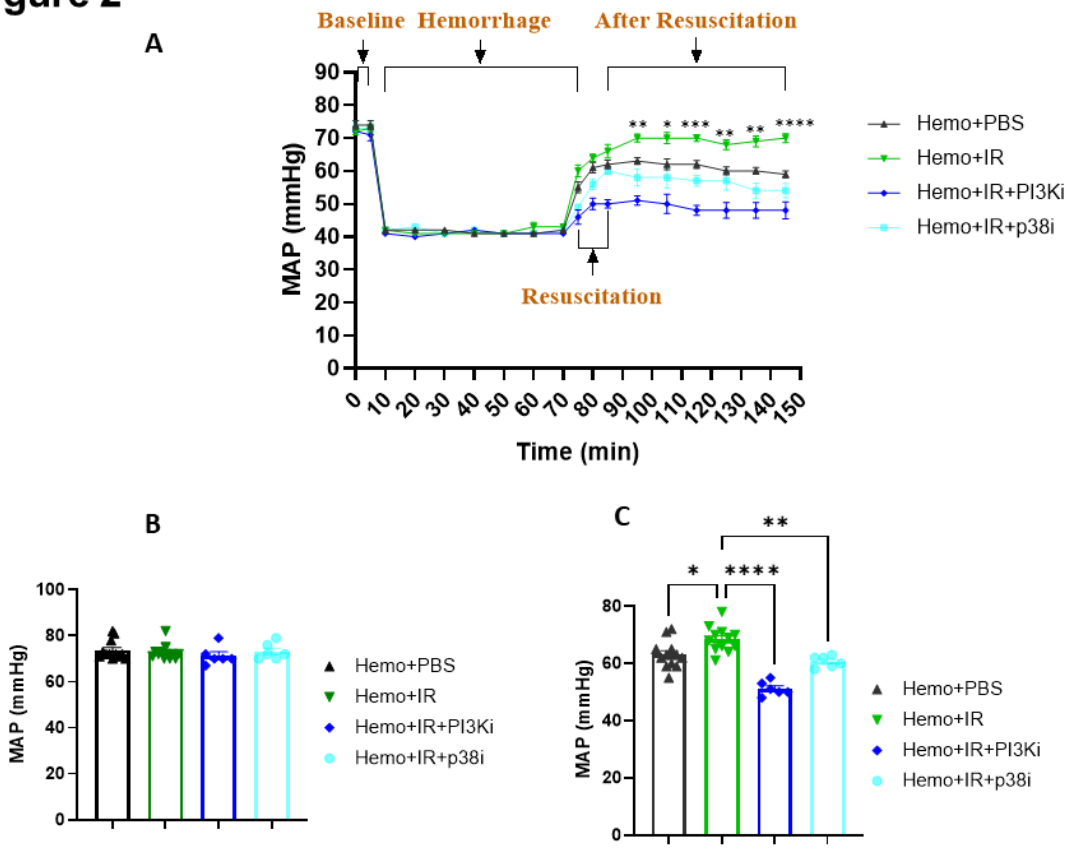

Figure 3

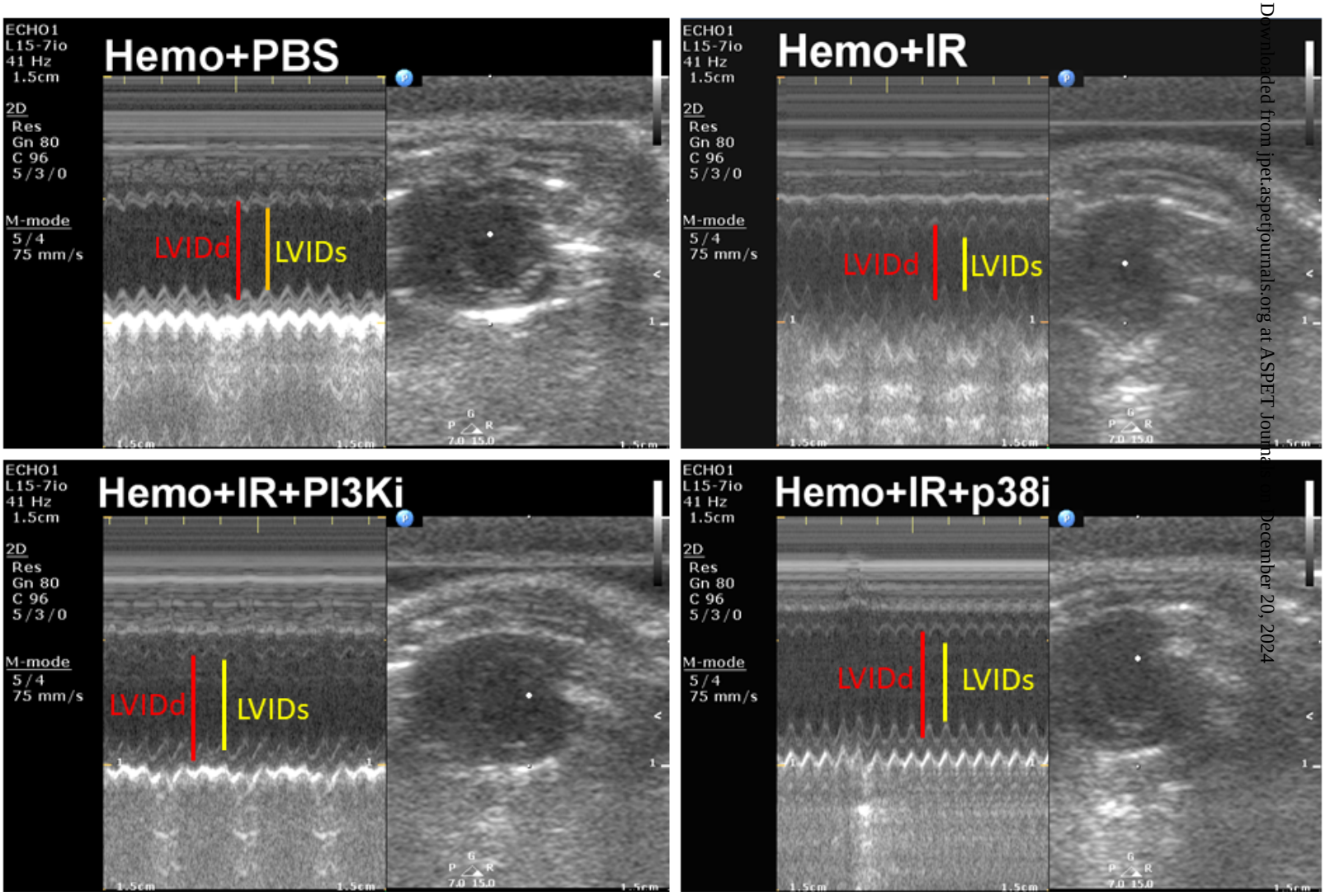

Figure 4

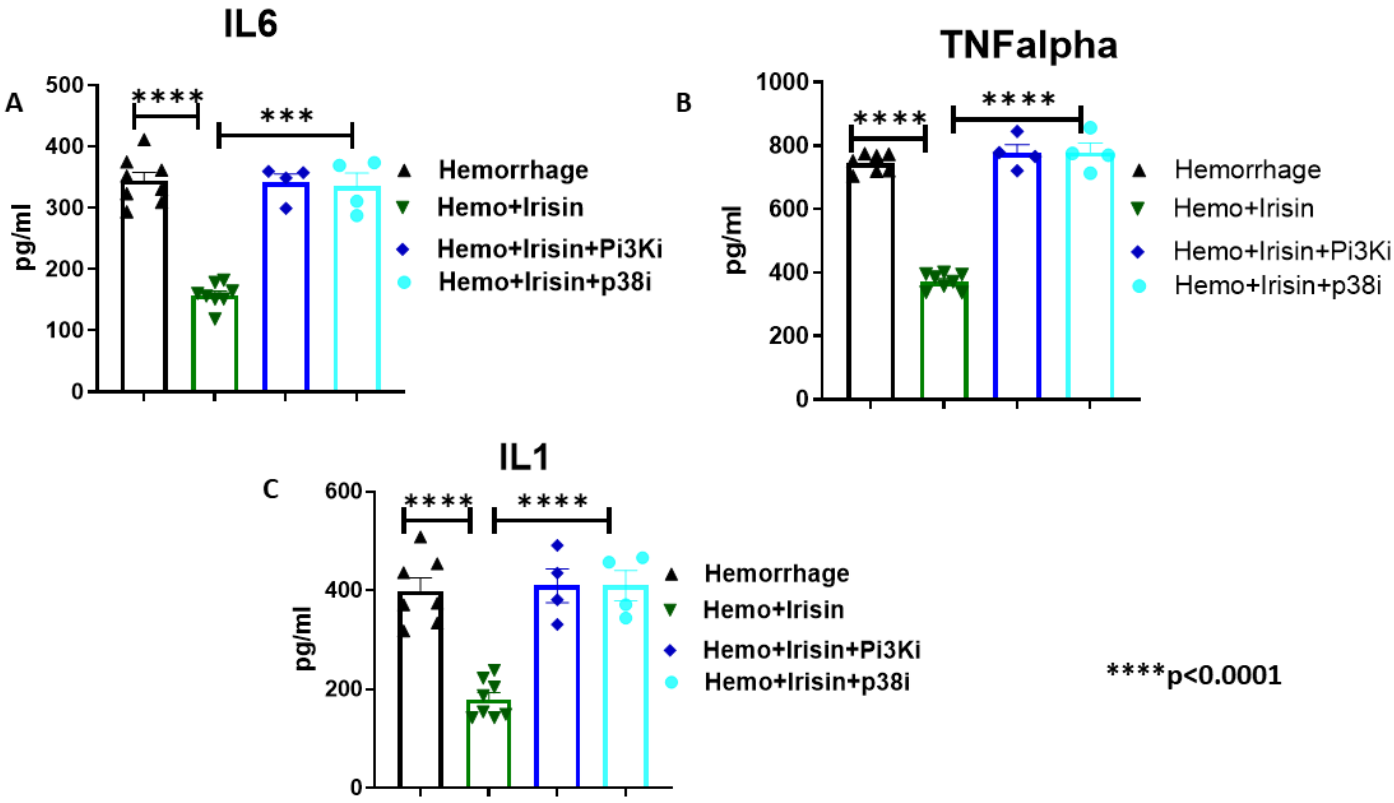

Figure 5

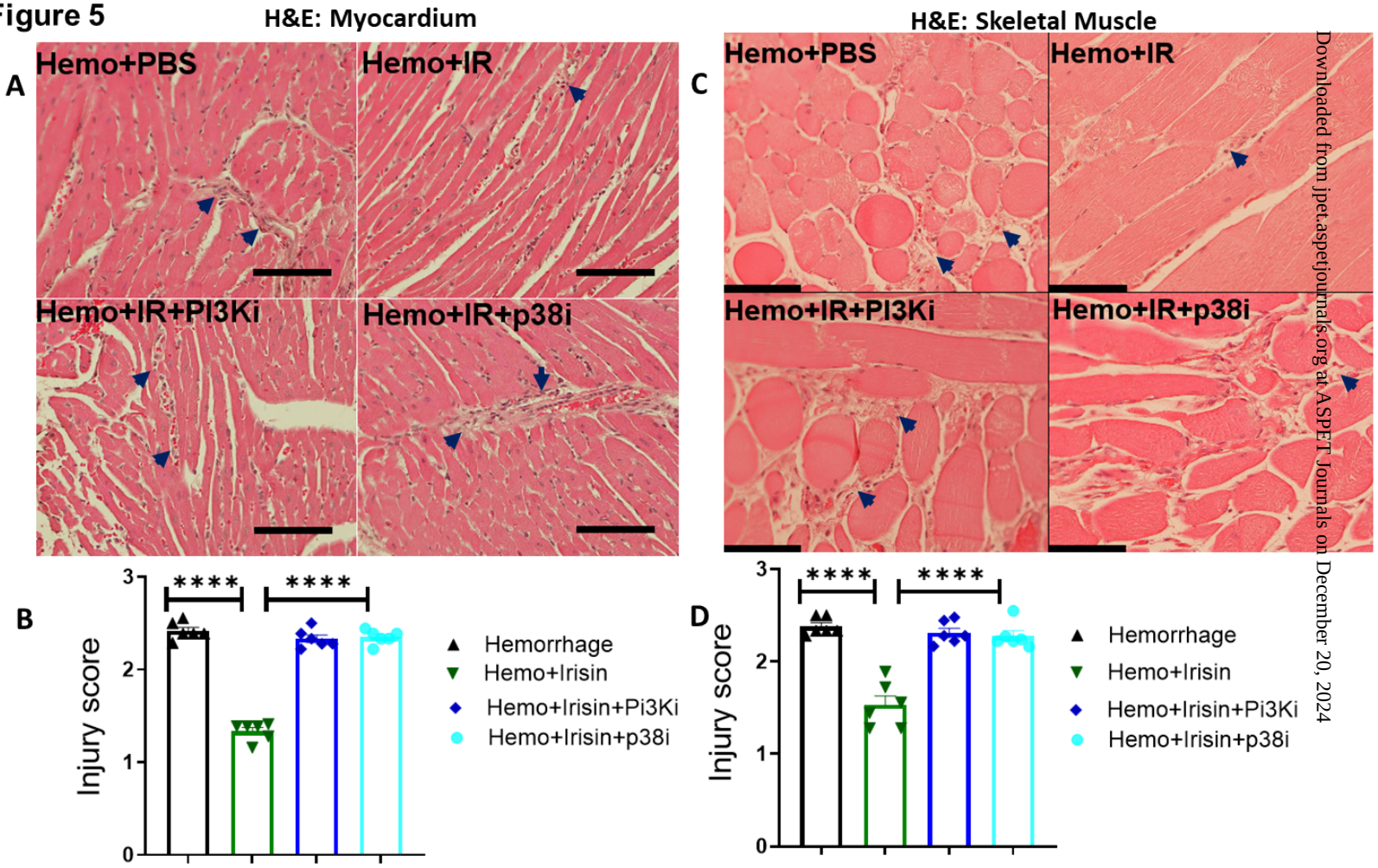

Figure 6

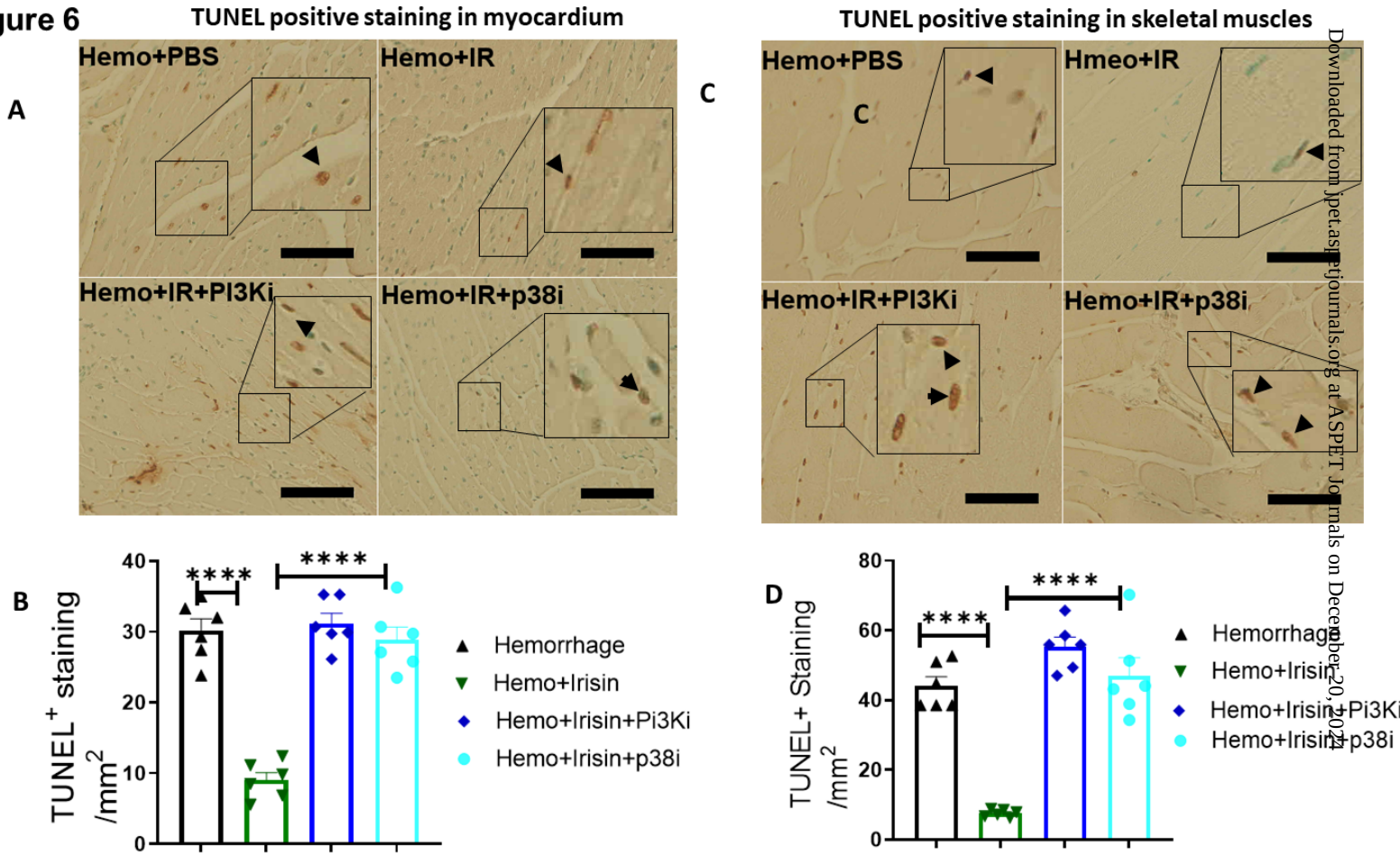

Figure 7

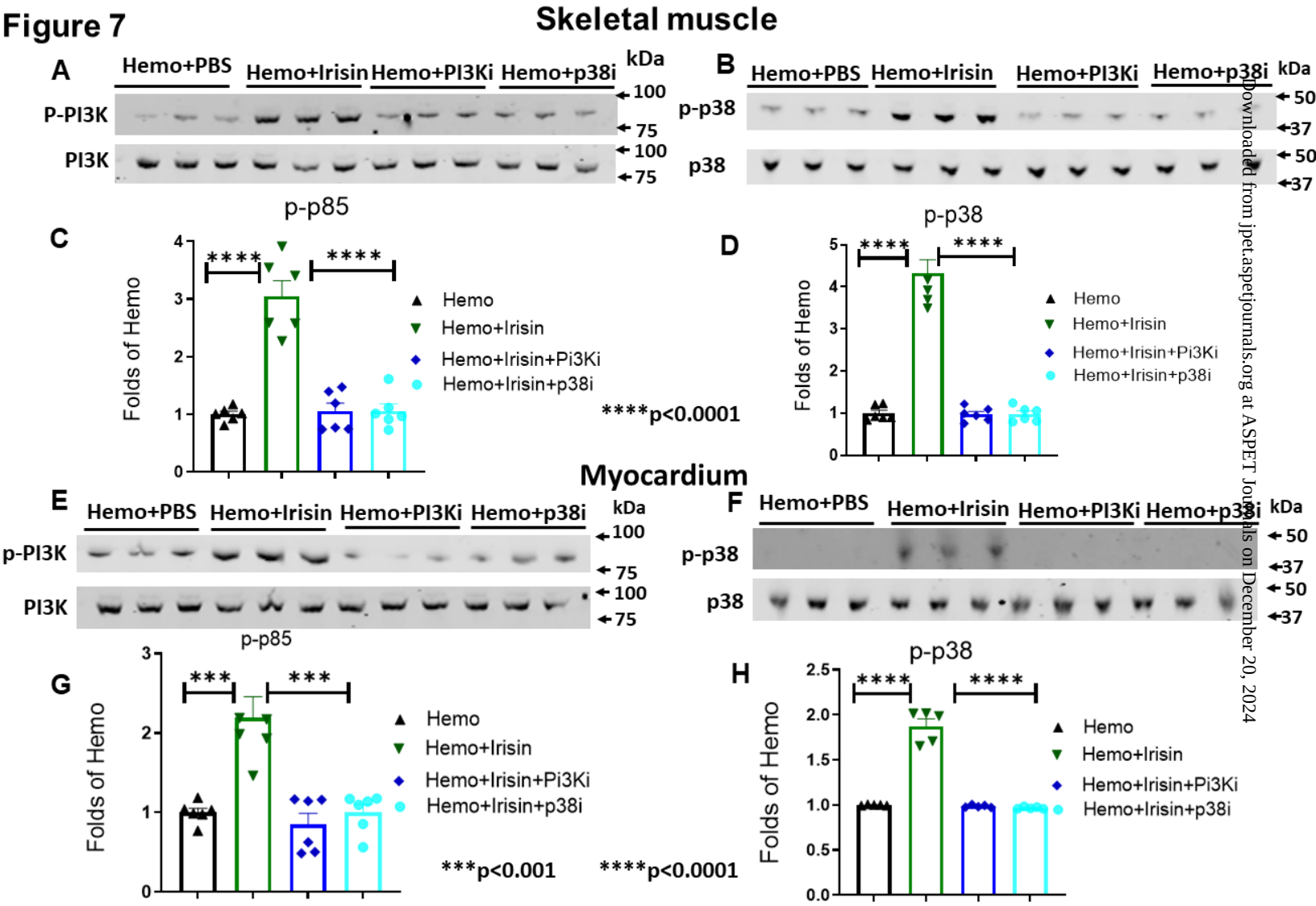

Figure 8